Magnetic structure in the zero-applied-field reentrant superconductor $ErNi_{1.96}Fe_{0.04}B_2C_{0.99}$

E. Alleno* and C. Godart
LCMTR-CNRS, ISCSA, 2-8 rue H. Dunant, 94320 Thiais, France

G. André
LLB, CEA-CNRS Saclay, 91191 Gif Sur Yvette Cedex, France

S. K. Dhar and S. M. Pattalwar
TIFR, Homi Bhabha Road, 400005 Mumbai, India

P. Bonville
DSM/DRECAM/SPEC, CEA Saclay, 91191 Gif Sur Yvette Cedex, France

R. Nagarajan and L. C. Gupta
TIFR, Homi Bhabha Road, 400005 Mumbai, India
(Received 22 May 2003; published 30 December 2003)

$ErNi_{1.96}Fe_{0.04}B_2C_{0.99}$ is superconducting at $T_c = 7.3\,K$ and is shown to partially reenter the normal state between 5.5 and 5.7 K in zero applied field by means of ac-susceptibility (χ'_{ac}) and resistivity measurements. Specific heat (C_p) measurements give a magnetic ordering temperature $T_N = 5.7 \pm 0.2\,K$. Powder neutron diffraction measurements showed that the Er^{3+} magnetic moments adopt below $T_N = 5.9 \pm 0.2\,K$ a transverse modulated structure along the *a* axis ($\mathbf{q} = 0.559\mathbf{a}^*$). Observation of third-order and fifth-order harmonics indicates a squaring of the structure at lower temperature ($8.2\mu_B$ at 1.4 K). Although even-order peaks could not be detected in the neutron data, a weak ferromagnetic transition at $T_{WFM} = 2.2\,K$ could be directly evidenced by magnetic susceptibility measurements and C_p measurements and indirectly evidenced in the thermal variations of the intensity of the first-order magnetic peaks ($I_\mathbf{q}$), the magnetic coherence length (ξ_m), and the magnetic wave vector ($\mathbf{q}$). The magnetic structure of $ErNi_{1.96}Fe_{0.04}B_2C_{0.99}$ is nearly identical to that of the parent compound $ErNi_2B_2C$. Precise comparison between the temperature variations of $I_\mathbf{q}$, ξ_m, and χ'_{ac} shows that the transverse $\mathbf{a}^*$-modulated magnetic structure is responsible for the reentrant behavior between 5.5 and 5.7 K. Although it is still pair breaking below 5.5 K, it coexists with superconductivity. ^{57}Fe Mössbauer spectra display no broadening in the temperature range where the reentrant behavior is observed, showing that the transferred hyperfine field at the Fe site, if any, is smaller than 2 kOe.

DOI: 10.1103/PhysRevB.68.214518 PACS number(s): 74.25.Ha, 74.70.Dd, 75.25.+z, 76.80.+y

I. INTRODUCTION

Four of the rare-earth (R) nickel-borocarbides RNi_2B_2C (R = Dy, Ho, Er, Tm (Ref. 1)) exhibit coexistence of a magnetic order with superconductivity. The magnetic moments originate from the localized $4f$ electrons of the rare earth, and they are exchange coupled by the RKKY interaction mediated by the conduction electrons. Many experiments have shown the interaction of superconductivity with the rare-earth-ordered sublattice in these compounds. One of its most dramatic manifestation is the local minimum observed close to the Néel temperature T_N in the upper critical field $H_{c2}(T)$ curve of $HoNi_2B_2C$,[1–4] $ErNi_2B_2C$,[1,5,6] and $TmNi_2B_2C$.[7] This effect is obviously related to the onset of magnetic order but the detailed mechanism is not yet fully understood.

In $HoNi_2B_2C$ ($T_c = 8.5\,K$), the minimum is attributed to the competition between superconductivity and a magnetic helical structure ($\mathbf{q} = 0.915\mathbf{c}^*$ (Refs. 8–10)) or to a partially determined magnetic structure ($\mathbf{q} = 0.585\mathbf{a}^*$, moment orientation unknown (Refs. 11–13)), or to both structures (Refs. 3 and 14), as they are both observed in the 5–6K temperature region where H_{c2} is depressed. Below 5 K the Ho^{3+} moments adopt a commensurate antiferromagnetic structure and H_{c2} increases again. Depending on the samples, a small magnetic field ranging from 0 to 700 Oe can drive this compound reentrant: it becomes superconducting at 8.5 K, reenters the normal state at 6 K, and superconductivity appears again at 5 K.[1–4]

$TmNi_2B_2C$ ($T_c = 11\,K$) exhibits below 1.5 K a transverse sine-wave structure with $\mathbf{q} = 0.094(\mathbf{a}^* + \mathbf{b}^*)$ in zero applied field.[15–17] In an applied field $H = 0.9$ T parallel to $\mathbf{a}$, this low-field structure transforms into a new structure with $\mathbf{q} = 0.48\mathbf{a}^*$ (Ref. 18) which is stable at least up to $H = H_{c2}(0\,K) = 2$ T. This high-field structure is potentially responsible for the depression of $H_{c2}(T)$ in $TmNi_2B_2C$ below $\sim 2\,K$.

$ErNi_2B_2C$ becomes superconducting at $T_c = 10.5\,K$ and the Er^{3+} moments adopt a transverse sine-wave structure [$\mathbf{q} = 0.553\mathbf{a}^*$, $\mathbf{m} \| \mathbf{b}$] at $T_N \approx 6$ K.[17,19–22] An incommensurate magnetic structure with $\mathbf{q} = 0.4–0.6\mathbf{a}^*$ is a common feature of these three magnetic RNi_2B_2C compounds and is caused by a nesting of their Fermi surface at this $\mathbf{q}$ vector.[23] Single-crystal measurements in $ErNi_2B_2C$ (Refs. 5 and 6) with an applied field H parallel to the $\mathbf{c}$ axis have shown that $H_{c2}(T)$ sharply decreases at 6 K (from 16 to 14 kOe for the best

samples) and starts increasing again at 5.5 K [$H_{c2}(2\,K) = 20$ kOe]. This effect is anisotropic because for $H\|(\mathbf{a},\mathbf{b})$, $H_{c2}(T)$ only exhibits an inflection point around 5 K. A similar feature is also observed in the lower-critical field $H_{c1}(T)$ curve.[24,25] The magnetic structure undergoes a transition from antiferromagnetism to weak ferromagnetism at $T_{\mathrm{WFM}} = 2.3\,K$,[21,26] which causes an increase of critical current due to enhanced pinning of the flux line lattice.[27]

Although superconductivity is more ''robust'' in $ErNi_2B_2C$ than in $HoNi_2B_2C$, a reentrant behavior can be observed in $ErNi_2B_2C$ by applying a field larger than $\sim$11 kOe.[5] Thus a direct and precise comparison between $H_{c2}(T)$ in $ErNi_2B_2C$ and neutron magnetic diffraction data usually obtained in zero applied field is difficult: T_N depends on the applied field in $ErNi_2B_2C$,[5] and even worse, in the case of $TmNi_2B_2C$ this would be misleading, as the zero-field magnetic structure is not the existing structure at H_{c2}. One way to overcome this difficulty is to depress globally the $H_{c2}(T)$ curve until its local minimum crosses the T axis and one observes a reentrant behavior in zero applied field. Of course, T_c is simutaneously depressed. This was obtained by Schmidt and Braun in $HoNi_2B_2C$ and in $ErNi_2B_2C$ (Ref. 28) by substituting cobalt on the nickel site: $HoNi_{1.99}Co_{0.01}B_2C$ and $ErNi_{1.935}Co_{0.065}Ni_2B_2C$ both exhibit reentrant superconductivity in zero applied field. Although magnetic neutron diffraction measurements were reported on nonsuperconducting $HoNi_{1.985}Co_{0.015}B_2C$,[29,30] no result was reported on the two above-mentionned reentrant compounds.

Iron doping also depresses T_c of the RNi_2B_2C compounds,[28,31,32] and it was expected that, similarly to cobalt, it would depress H_{c2} and induce reentrant superconductivity in zero applied field in $ErNi_{2-x}Fe_xB_2C$. Therefore, we report in this paper that $ErNi_{1.96}Fe_{0.04}B_2C_{0.99}$ is a reentrant superconductor ($T_c = 7.3\,K$, $T_N = 5.9\,K$, $T_{\mathrm{WFM}} = 2.2\,K$) in zero applied field. As the determination of the magnetic structures of $ErNi_{1.96}Fe_{0.04}B_2C_{0.99}$ is of high interest to look for correlations with its exotic superconducting properties, we carried out neutron powder diffraction. Accordingly, we also performed ^{57}Fe Mössbauer spectroscopy measurements to examine if the magnetic structure present in the reentrant region leads to the introduction of a hyperfine field at the Fe probe.

II. EXPERIMENT

A $Ni_{0.98}Fe_{0.02}$ master alloy (Ni 99.9% and Fe 99.9%) was first melted in an induction furnace. Three 2.5-g $ErNi_{1.96}Fe_{0.04}$ $^{11}B_2C_{0.99}$ polycrystalline samples labeled A, B, and C were prepared by melting proper amounts of Er (99.9%), ^{11}B (Eurisotop, 99.8% chemically pure, 97.5% isotopically enriched), carbon (99.7%), and of the Ni-Fe master alloy in an arc furnace under Ar atmosphere. ^{11}B isotope was used to reduce the neutron absorption caused by ^{10}B in natural boron. The resulting buttons were melted and flipped over several times to ensure a good homogeneity. Weight losses were less than 1%. The samples were annealed for 6 days at 1100 °C and subsequently characterized by powder x-ray diffraction and ac-susceptibility measurements. Last, they were ground to a fine powder and mixed together to make a $\sim$7-g sample large enough to ensure a good neutron diffraction signal. Similarly a $ErNi_{1.96}$ $^{57}Fe_{0.04}B_2C_{0.98}$ sample (labeled D) was specifically synthesized with ^{57}Fe for the Mössbauer spectroscopy measurements. Our samples were purposely melted with a carbon content slightly (1%–2%) below stoichiometry because it favors the reentrant behavior in zero applied field as already observed in $HoNi_2B_2C_y$.[33]

Powder x-ray diffraction (Brüker D8, Cu $K\alpha$ radiation, Si NBS SRM640 as reference) showed that in each sample, $ErNi_{1.96}Fe_{0.04}B_2C_{0.99}$ crystallizes in the $LuNi_2B_2C$ structure type (space group $I4/mmm$) with lattice parameters $a = 3.501(1)$ Å and $c = 10.563(2)$ Å in samples $A-C$ and $a = 3.501(1)$ and $c = 10.560(2)$ in sample D. Here 3% ErB_2C_2 and 1% $Er_2Ni_3B_6$ were detected as impurity phases in samples $A-C$ and sample D, respectively. Electron probe microanalysis performed on other $ErNi_{2-x}Fe_xB_2C$ samples ($x = 0.04$, 0.05, 0.1, 0.2) showed that iron is uniformly distributed in the matrix and that it follows a solid-solution behavior in this concentration range.

ac-susceptibility measurements were performed on a homebuilt system with an amplitude of $\sim$1 Oe applied field at 331 Hz. Resistivity was measured using a four-probe setup in applied dc current mode ($j = 20$ A/cm^2).

Magnetic susceptibility measurements were performed in a commercial superconducting quantum interference device (SQUID) magnetometer (Quantum Design) under 500 Oe after zero-field cooling.

Specific heat measurements were carried out on a homemade semiadiabatic heat-pulse-type calorimeter.

Mössbauer measurements were made using a ^{57}Co:Rh source mounted on a triangular velocity drive in the temperature range 4.2–8 K. The isomer shift measured with this source must be shifted by 0.114 mm/s to obtain values with respect to the standard α-Fe.

The neutron experiment was performed at the Laboratoire Léon Brillouin (CEA-CNRS, Saclay) using the two-axis multidetector G4.1 diffractometer with $\lambda = 2.427$ Å and $7° \leqslant 2\theta \leqslant 87°$. The sample was held in a vanadium can ($R = 4$ mm) and placed in a He cryostat. Neutron powder diffractograms were acquired as a function of temperature in the [1.4–10 K] range. Rietveld refinements of the nuclear and magnetic structures were performed with the help of the program FULLPROF.[34] The nuclear scattering lengths published by Sears[35] were used and the neutron linear absorption coefficient was computed ($\mu R = 1.5$). The scale factors, the lattice parameters a and c, the Lorentzian peak broadening caused by the finite coherence length (Thomson-Cox-Hastings peak profile[36]), the magnetic moments, and propagation vectors were refined parameters. The boron z coordinate, the Gaussian instrumental peak broadening parameters, the site occupation factors, and the thermal displacement parameters were held fixed.

III. RESULTS AND DISCUSSION

A. ac-susceptibility, resistivity, and specific heat measurements

We have shown in a recent work on $ErNi_{2-x}Fe_xB_2C$ ($x < 0.2$) (Ref. 37) that substitution on the Ni site by Fe

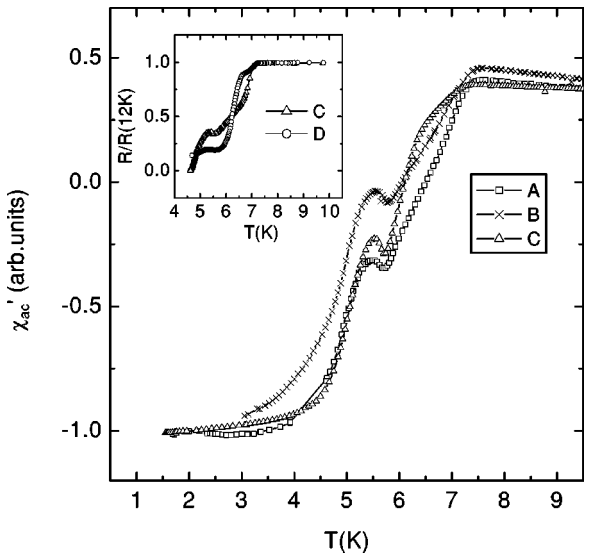

FIG. 1. ac Susceptibility of the three $ErNi_{1.96}Fe_{0.04}$ $^{11}B_2C_{0.99}$ samples used in our neutron diffraction experiment. Inset shows the resistivity of one of these samples (C) and of the ^{57}Fe Mössbauer sample (D).

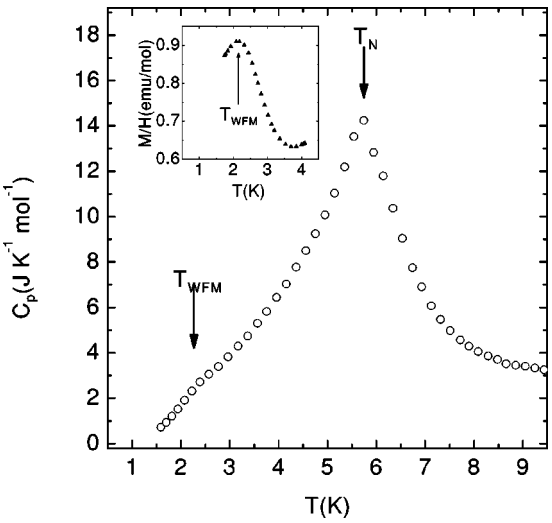

FIG. 2. Specific heat (C_p) of $ErNi_{1.96}Fe_{0.04}B_2C_{0.99}$ as a function of temperature. In the inset is displayed a magnetic susceptibility measurement in $ErNi_{1.96}Fe_{0.04}B_2C_{0.99}$ at low temperature.

strongly decreases T_c at an average rate of $dT_c/dx = -100$ K/mol(Fe). Diminution of the density of states $[N(\varepsilon)]$ at the Fermi level (ε_f) appears to be the main reason for this T_c depression because the smaller electron density (Fe has two electrons fewer than Ni) shifts the Fermi level away from the maximum of $N(\varepsilon)$ nearly attained in the pure compound.[38–40] The real part of the normalized ac susceptibility (χ'_{ac}) measured on our three $ErNi_{1.96}Fe_{0.04}B_2C_{0.99}$ samples is plotted as a function of temperature in Fig. 1. The three curves are nearly identical. The decrease of χ'_{ac} at $T_c = 7.3$ K (onset) corresponds to the superconducting transition, which occurs at 10.5 K in $ErNi_2B_2C$. Here χ'_{ac} increases at 5.7 K and diminishes again at 5.5 K. Therefore, $ErNi_{1.96}Fe_{0.04}B_2C_{0.99}$ partially reenters the normal state at 5.7 K and regains superconductivity at 5.5 K. The effect is reproducible and its magnitude compares well with what was observed in $ErNi_{1.935}Co_{0.065}B_2C$.[28] Approximately 50% of the samples (by volume) is not superconducting at 5.5 K. The resistivity curve plotted in the inset of Fig. 1 was measured on sample C. Its behavior correlates with features seen in the $\chi'_{ac}(T)$ curves, although most likely a difference of calibration of the thermometers causes a small temperature shift (-0.1 K) relative to the $\chi'_{ac}(T)$ curves. Sample *D* also displays a resistivity curve very similar to the curve of sample C with a local maximum, although less pronounced, at 5.4 K. All these experimental data demonstrate that $ErNi_{1.96}Fe_{0.04}B_2C_{0.99}$ is at least partially a reentrant superconductor between 5.5 and 5.7 K in zero aplied field.

From magnetic susceptibility measurements, we obtained an antiferromagnetic ordering temperature $T_N = 5.9 \pm 0.2$ K for $ErNi_{1.96}Fe_{0.04}B_2C_{0.99}$.[37] This shows that for x(Fe) < 0.05, T_N weakly depends on x(Fe) ($T_N = 6$ K in $ErNi_2B_2C$). Here, we present in Fig. 2 specific heat measurements ($H = 0$) as a function of temperature $[C_p(T)]$ in $ErNi_{1.96}Fe_{0.04}B_2C_{0.99}$ which confirm this view. A large peak corresponding to the antiferromagnetic transition and a shoulder corresponding to the weak ferromagnetic transition are clearly seen at, respectively, $T_N = 5.7 \pm 0.2$ K and $T_{WFM} = 2.2 \pm 0.2$ K (see arrows in Fig. 2). Magnetic susceptibility measurements on $ErNi_{1.96}Fe_{0.04}$ $^{11}B_2C_{0.99}$ also displays a large peak at 2.2 K (see the inset of Fig. 2) and confirm that iron doping does not smear off the weak ferromagnetic transition. The specific heat change associated with the superconducting transition at 7.3 K is not seen in our data because the magnetic contribution to C_p is still very high at T_c. No other magnetic transition could be detected either by magnetic susceptibility or specific heat measurements.

B. Neutron diffraction measurements

Portions of the experimental diffraction patterns of $ErNi_{1.96}Fe_{0.04}B_2C_{0.99}$ obtained at 10.0, 6.0, and 1.4 K are plotted in Fig. 3. At 10 K, only the nuclear peaks are visible and our Rietveld refinement confirms the x-ray diffraction results—i.e., that $ErNi_{1.96}Fe_{0.04}B_2C_{0.99}$ adopts the $LuNi_2B_2C$ structure type ($I4/mmm$). Magnetic peaks are already visible at 8 K and fully develop between 6 and 7 K. They can easily be indexed at $T = 6.0$ K by the wave vector $\mathbf{q} = 0.566\mathbf{a}^*$ or equivalently by $\mathbf{q} = 0.566\mathbf{b}^*$. Third-order peaks ($3\mathbf{q}$) and fifth-order peaks ($5\mathbf{q}$) can also be observed respectively below ~ 5 and ~ 3 K. Higher orders were observed in single-crystalline $ErNi_2B_2C$,[20] but were not detected in our case. Neither even-order peaks corresponding to the weak ferromagnetic structure ($T_{WFM} = 2.2$ K) nor intensity changes of the nuclear peaks could be observed in the scanned temperature range [1.4–10 K]. As the $2\mathbf{q}$ peaks are an order of magnitude smaller than the $3\mathbf{q}$ peaks,[21] they are obviously beyond the detection limit of the G4.1 diffractometer. The magnetic peaks intensity are well fitted by a transverse sine-wave structure with $\mathbf{m} \| \mathbf{b}$ (or equivalently $\mathbf{q} \| \mathbf{b}^*$ and $\mathbf{m} \| \mathbf{a}$) adopted by the Er^{3+} ions. Attempts to model the magnetic peaks intensity with a Er^{3+} helimagnetic structure [$\mathbf{q} = 0.566\mathbf{a}^*$, $\mathbf{m} \| (\mathbf{b}, \mathbf{c})$] resulted in reliability factors

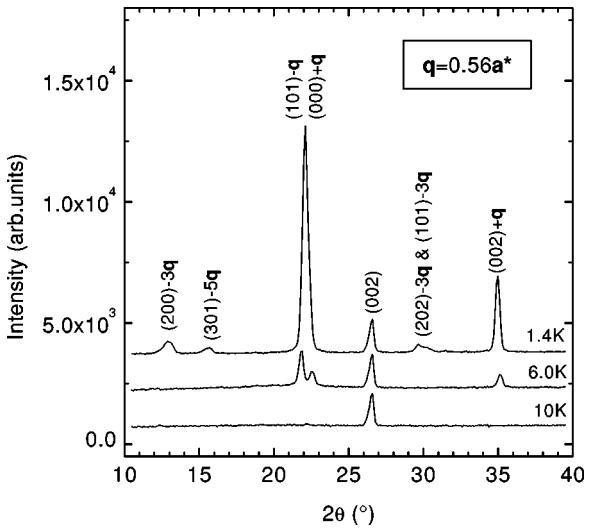

FIG. 3. Experimental diffraction patterns of $ErNi_{1.96}Fe_{0.04}{}^{11}B_2C_{0.99}$ at 1.4, 6, and 10 K and proposed peak indexation.

multiplied by a factor of 2. Refinements involving a small moment on the Ni/Fe site showed that it is zero within experimental error. The occurrence of third and fifth harmonics when temperature is lowered below 5.2 K corresponds to a squaring of the sine wave. No other magnetic structure was observed in the explored temperature range [1.4–10 K].

Figure 4 shows the good quality Rietveld refinement ($R_p = 5.1\%$) obtained on the 1.4-K pattern. Six contributions to the pattern were taken into account: the $ErNi_{1.96}Fe_{0.04}B_2C_{0.99}$ nuclear and magnetic phases ($\mathbf{q} = 0.559\mathbf{a}^*$, $3\mathbf{q}$, and $5\mathbf{q}$) and the nuclear and antiferromagnetic contributions of the secondary phase (3%) ErB_2C_2 ($T_N = 13$ K).[41] Compared to room-temperature values, the *a* lattice parameter of $ErNi_{1.96}Fe_{0.04}B_2C_{0.99}$ decreases from 3.500 to 3.497 Å at 1.4 K and the *c* lattice parameter increases from 10.563 to 10.567 Å. The lattice parameters are constant in the temperature range [1.4–10 K]. The propagation vector $\mathbf{q} = 0.559\mathbf{a}^*$ is very close to the $0.553\mathbf{a}^*$ value found in the works of Zarestky *et al.*[20] and of Lynn *et al.*[17] both on $ErNi_2B_2C$. These small differences could be accounted for by changes in the electronic structure at the Fermi level caused by the Fe doping as this modulated structure with $\mathbf{q} \sim (0.5-0.6)\mathbf{a}^*$ present in several RNi_2B_2C (R = Gd, Tb, Er, Ho, Tm) compounds is attributed to a nesting of the Fermi surface.[23] The magnitude at 1.4 K of the three Fourier components of the Er^{3+} moments are $m_1 = 10.4(1)\mu_B$, $m_3 = 3.4(1)\mu_B$, and $m_5 = 1.9(1)\mu_B$. The ratios $m_3/m_1 = 0.33$ and $m_5/m_1 = 0.18$ are close to the 1/3 and 1/5 ratio expected for a perfectly squared structure. Making this assumption at 1.4 K, these Fourier components would correspond to a squared moment of $\sim 8.2\mu_B$. The same value was found in a previous ^{166}Er Mössbauer spectroscopy study of $ErNi_2B_2C$,[42] and it is also very similar to the $8\mu_B$ found by Zarestky *et al.*[20] It is, however, larger than the $7.2\mu_B$ found by Lynn *et al.*[17,19] but this discrepancy may be well accounted for by small composition differences such as the carbon content which has been shown to be very influential on the value of the magnetic moment of the rare earth in the RNi_2B_2C series.[33,43] The high degree of similarity between the characteristic parameters of the two magnetic structures observed in $ErNi_{1.96}Fe_{0.04}B_2C_{0.99}$ and $ErNi_2B_2C$ lets us conclude that both are nearly identical. The effect of Fe doping on the magnetic parameters of $ErNi_2B_2C$ is very weak: $\mathbf{q}$ only is slightly affected while the other parameters remain constant. Superconductivity is more drastically affected.

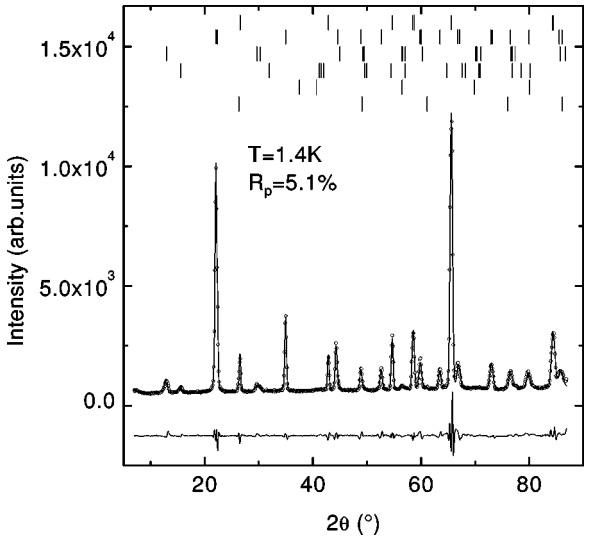

FIG. 4. Experimental (circles) and calculated (line) diffraction pattern of $ErNi_{1.96}Fe_{0.04}B_2C_{0.99}$ at 1.4 K. The top six sets of small vertical lines correspond to the Bragg positions of the six contributions to the pattern. From top to bottom: $ErNi_{1.96}Fe_{0.04}B_2C_{0.99}$ nuclear and magnetic phases ($\mathbf{q} = 0.559\mathbf{a}^*$, $3\mathbf{q}$, and $5\mathbf{q}$) and ErB_2C_2 (3%) nuclear and antiferromagnetic phases. The bottom line is the difference between experience and calculation. $R_p = 5.1\%$.

Figure 5(a) shows the evolution with temperature of the magnetic integrated intensities of the peaks indexed (000) $+\mathbf{q}$ and (101) $-\mathbf{q}$, the (200) $-3\mathbf{q}$ peak, and the (301) $-5\mathbf{q}$ peak respectively labeled $I_{\mathbf{q}}$, $I_{3\mathbf{q}}$, and $I_{5\mathbf{q}}$. Of course, as expected, the three components increase when the temperature decreases. A power law fit of $I_{\mathbf{q}}$ between 1.4 and 5.8 K yields $T_N = 5.9 \pm 0.2$ K. This T_N value is identical to the 5.9 K derived from magnetic susceptibility measurements and very close to the 5.7 K obtained from our $C_p(T)$ experiment. $T_N = 5.9$ K (Ref. 20) and $T_N = 6.0$ K (Ref. 21) were previously determined by neutron diffraction experiments in $ErNi_2B_2C$. This confirms that T_N weakly depends on Fe doping in this ''low-concentration'' range. Above 5.9 K, pretransitional scattering is observed at least up to 8 K. Here $I_{3\mathbf{q}}$ and $I_{5\mathbf{q}}$ respectively develop below 5.2 K and 3.6 K. However, these two components might already exist just above these temperatures, as their diffraction peaks are initially small and broad and might lay below the detection limit of our experiment. As already mentioned, refinements showed that the structure is nearly fully squared at 1.4 K.

The temperature variations of the magnitude of the propagation vector ($\mathbf{q}$) are plotted in Fig. 5(b). It significantly varies (-1.4%) in the scanned temperature range. Above 7 K,

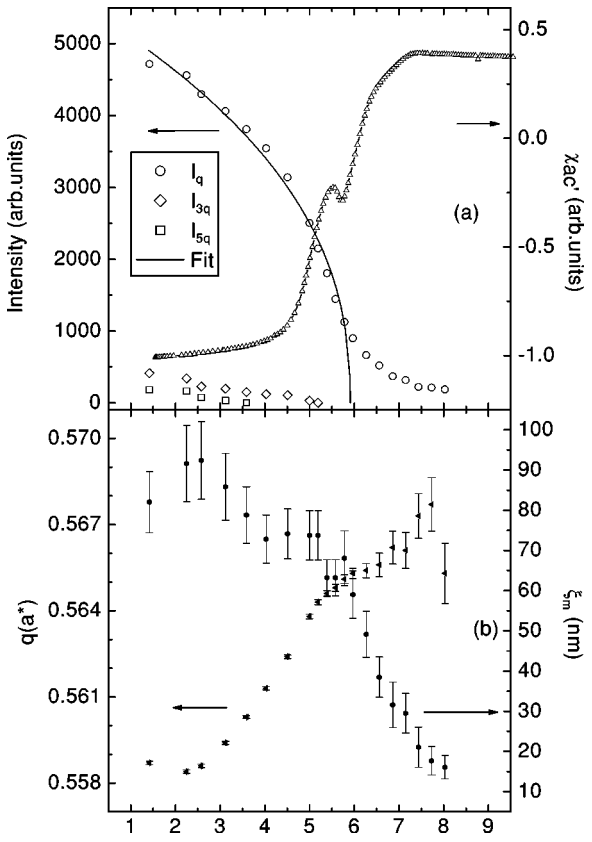

FIG. 5. (a) Thermal variations of the magnetic integrated intensities of the first, third, and fifth order ($I_{\mathbf{q}}$, $I_{3\mathbf{q}}$, and $I_{5\mathbf{q}}$) and of χ'_{ac}. (b) Thermal variations of the magnetic wave vector length (q) and of the magnetic coherence length ξ_m.

it is difficult to attribute a sign to its variations as **q** rather fluctuates around a mean value ($0.566|\mathbf{a}^*|$). Between 7 and 2.2 K, it decreases with temperature from $0.566|\mathbf{a}^*|$ to $0.558|\mathbf{a}^*|$. Below 2.2 K, it remains constant or slightly increases. At 5 K ($\mathbf{q}=0.565|\mathbf{a}^*|$) a change of slope is noticeable. Although the absolute values are slightly different, this temperature dependence is very similar to what was observed by Choi *et al.* in $ErNi_2B_2C$.[21] A mean-field model involving spin-slip structures explains these thermal variations of the modulation vector in $ErNi_2B_2C$.[44] It could most probably also be applied in the present case.

From the Lorentzian broadening of the magnetic first-order peaks (Y in radians), a magnetic coherence length (ξ_m) can be deduced using the following equation: $\xi_m = 2\lambda/\pi Y$. It is also plotted as a function of temperature in Fig. 5(b) and its variations are also instructive as they are qualitatively very similar to the variations of $I_{\mathbf{q}}$. Between 8 and $\sim$6.5 K, in the preorder regime, it increases slower than between $\sim$6.5 and 5.6–5.8 K where the long-range magnetic order develops. Below 5.6–5.8 K, ξ_m increases until $T_{\mathrm{WFM}} = 2.2$ K where it decreases. The maximum value of ξ_m at T_{WFM} is not caused by a limited instrumental resolution but is intrinsic. On the contrary, the nuclear peaks width is limited by the instrumental resolution and it is impossible to extract a nuclear coherence length and to compare it with the magnetic coherence length. $I_{\mathbf{q}}(T)$ also seems to level off

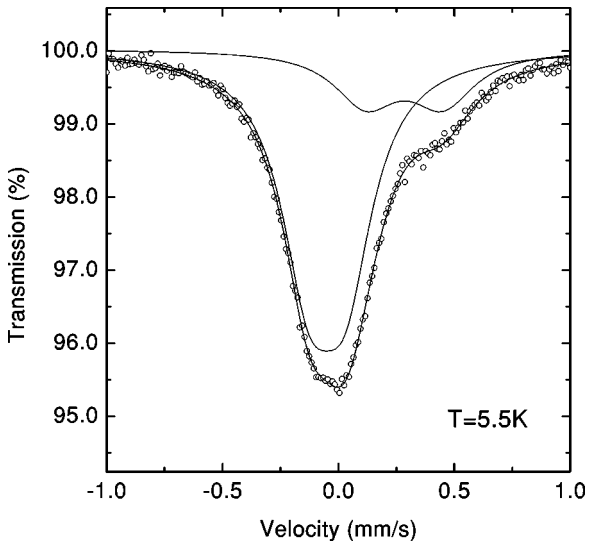

FIG. 6. ^{57}Fe Mössbauer absorption spectrum in $ErNi_{1.96}{}^{57}Fe_{0.04}B_2C_{0.98}$ at 5.5 K.

below 2.2 K as it is smaller than expected from the power law fit and a reverse effect is seen in the $\mathbf{q}(T)$ curve which reaches a minimum or a plateau at T_{WFM}. Similar effects can also be noticed at T_{WFM} in the $I_{\mathbf{q}}(T)$ and $\mathbf{q}(T)$ data published by Choi *et al.*[21] in $ErNi_2B_2C$. Therefore, our neutron diffraction measurements indirectly show that $ErNi_{1.96}Fe_{0.04}B_2C_{0.99}$ undergoes a transition to weak ferromagnetism.

C. ^{57}Fe Mössbauer spectroscopy

The ^{57}Fe Mössbauer spectra in $ErNi_{1.96}{}^{57}Fe_{0.04}B_2C_{0.98}$, recorded between 4.2 and 8 K show no thermal variation. In particular, no line broadening is observed in this temperature range, showing that any transferred hyperfine field at the Fe probe in the reentrant region ($5<T<6$ K) is smaller than 2 kOe. Figure 6 shows that the spectra consist of two quadrupolar doublets: the dominant one (75% relative intensity) has an isomer shift of 0.06 mm/s with respect to α-Fe and a small quadrupolar splitting of 0.15 mm/s. It most probably corresponds to Fe substituted at the Ni site. The minority component (25%) has an isomer shift of 0.38 mm/s and a larger quadrupolar splitting of 0.35 mm/s. Past Er, Tm, and Fe Mössbauer studies of RNi_2B_2C compounds showed the presence of a minority component in the spectra.[42,43,45,46] This component is most likely originating from distorted Fe or rare-earth sites close to carbon vacancies[42,43] which affect the crystalline electric field. Our sample is indeed carbon deficient (0.98). Our data seem to contradict the result of Ref. 45, where a small hyperfine field ($\sim$3 kOe) was reported in the reentrant region [5–6 K] of $HoNi_{1.98}Fe_{0.02}B_2C$, unless the transferred field in $ErNi_{1.96}{}^{57}Fe_{0.04}B_2C_{0.98}$ is smaller than 2 kOe. Our result is, however, consistent with what we reported in $HoNi_{1.99}Fe_{0.01}B_2C$ (Ref. 46) and what was obtained in $ErNi_{1.98}Fe_{0.02}B_2C$ by authors of Ref. 45: in both cases, no transferred field was observed. We conclude that a reentrant behavior in zero applied field can be observed while no transferred field can be detected at the Ni/Fe site.

D. Discussion

The $\chi'_{ac}(T)$ curve of sample A is also plotted in Fig. 5 to allow correlation between the reentrant behavior and the thermal variations of the microscopic magnetic parameters in $ErNi_{1.96}Fe_{0.04}B_2C_{0.99}$. The superconducting order parameter starts increasing ($T_c = 7.3$ K) in the critical scattering regime between 8 K and $T_N = 5.9$ K where $I_{\mathbf{q}}$ and ξ_m slowly increase. This temperature range most likely corresponds to short-range magnetic ordering of the material but one cannot exclude long-range-ordered magnetic regions spread in a dominantly paramagnetic material. This question is of course intimately linked to the problem of determining the order of the magnetic transition in $ErNi_2B_2C$ and $ErNi_{1.96}Fe_{0.04}B_2C_{0.99}$ which according to us remains open. Past neutron studies[17,19,20] of $ErNi_2B_2C$ did not reveal any thermal hysteresis of the magnetic intensities. This would lead us to conclude that the transition is of second order type. However, our ^{166}Er Mössbauer spectroscopy work on $ErNi_2B_2C$ (Ref. 42) gave strong support to a first-order transition. Either superconductivity develops in already short-range-ordered regions or only in paramagnetic regions spatially separated from the magnetically ordered region of the material. It is therefore difficult to conclude whether the magnetic structure is detrimental or not to superconductivity in the critical scattering regime. At $T_N = 5.9$ K, $I_{\mathbf{q}}$ increases faster and the **a**-modulated magnetic structure grows. This nearly coincides with the beginning of the reentrant behavior at 5.7 K. There is also a clear correlation with the variations of $\xi_m(T)$ which saturates at 5.6 K. Hence, the **a***-modulated magnetic structure is detrimental to the superconductivity in the temperature range 5.5–5.7 K. Several models[10,47] predict that in a antiferromagnetic superconductor, the depression of the electron-phonon coupling parameter (λ) is proportional to the magnetic order parameter (m): $\lambda' = [1 - \text{const} \times m(T)]$. These models can explain how below T_N, the rapidly growing m depresses λ enough to drive the system, at least partially, back to a normal state. However, one has to be cautious because these models based on a mean-field theory are used in a temperature range close to T_N where critical phenomena are certainly at work. Below 5.5 K, superconductivity reappears because the superconducting order parameter keeps on increasing while the magnetic order parameter begins to saturate. Indeed, the magnetic moment derived from our data is already $6.7\mu_B$/Er at 5.5 K ($8.2\mu_B$/Er at 1.4 K) and $\xi_m(T)$ does not increase anymore. This implies that although the transverse **a**-modulated magnetic structure is detrimental to superconductivity, its magnetic pair-breaking energy obviously becomes smaller below 5.5 K than the superconducting condensation energy and it coexists with superconductivity. In $ErNi_2B_2C$, $H_{c2}(T)$ is most probably much larger (20 kOe at 2 K) than in $ErNi_{1.96}Fe_{0.04}B_2C_{0.99}$ and no signature of the magnetic transition is visible in ac-susceptibility or resistivity measurements in low magnetic field. However, as already described in the Introduction, $H_{c1}(T)$ and $H_{c2}(T)$ curves of $ErNi_2B_2C$ are also depressed just below T_N by the transverse modulated structure which remains pair breaking even at lower temperature. Consequently, H_{c2} never recovers to the value of the nonmagnetic reference compound $LuNi_2B_2C$ (80 kOe at 2 K).[48] This contradicts previous results which had concluded that the transverse modulated structure is not detrimental[20] to superconductivity in $ErNi_2B_2C$.

IV. CONCLUSION

We showed that $ErNi_{1.96}Fe_{0.04}B_2C_{0.99}$ is a reentrant superconductor in zero applied field. Parts of the sample reenters the normal state between 5.5 and 5.7 K. The Er^{3+} magnetic moments adopt below $T_N = 5.9$ K the same structure as in $ErNi_2B_2C$, i.e., a transverse modulated structure ($\mathbf{q} = 0.559\mathbf{a}^*$), which squares at lower temperature and transforms to weak ferromagnetism below $T_{WFM} = 2.2$ K. This antiferromagnetic ordering is at the origin of the reentrant behavior below T_N and is detrimental to superconductivity even at lower temperature, despite their coexistence. No transferred field was detected at the Ni/Fe site in the reentrant temperature region.

ACKNOWLEDGMENTS

Part of this work was supported by Indo-French IFCPAR Contract No. 1808-1. We thank E. Leroy for EPMA measurements.

*Corresponding author. Electronic address: eric.alleno@glvt-cnrs.fr

[1] H. Eisaki, H. Takagi, R. J. Cava, B. Batlogg, J. J. Krajewski, W. F. Peck, K. Mizuhashi, J. O. Lee, and S. Uchida, Phys. Rev. B **50**, 647 (1994).
[2] M. S. Lin, J. H. Shieh, Y. B. You, W. Y. Guan, H. C. Ku, H. D. Yang, and J. C. Ho, Phys. Rev. B **52**, 1181 (1995).
[3] K. Krug, M. Heinecke, and K. Winzer, Physica C **267**, 321 (1996).
[4] K. D. D. Rathnayaka, D. G. Naugle, B. K. Cho, and P. C. Canfield, Phys. Rev. B **53**, 5688 (1996).
[5] B. K. Cho, P. C. Canfield, L. L. Miller, D. C. Johnston, W. P. Beyermann, and A. Yatskar, Phys. Rev. B **52**, 3684 (1995).
[6] S. L. Bud'ko and P. C. Canfield, Phys. Rev. B **61**, 14 932 (2000).
[7] B. K. Cho, M. Xu, P. C. Canfield, L. L. Miller, and D. C. Johnston, Phys. Rev. B **52**, 3676 (1995).
[8] T. E. Grigereit, J. W. Lynn, Q. Huang, A. Santoro, R. J. Cava, J. J. Krajewski, and W. F. Peck, Phys. Rev. Lett. **73**, 2756 (1994).
[9] A. I. Goldman, C. Stassis, P. C. Canfield, J. Zarestky, P. Dervenagas, B. K. Cho, D. C. Johnston, and B. Sternlieb, Phys. Rev. B **50**, 9668 (1994).
[10] A. Amici, P. Thalmeier, and P. Fulde, Phys. Rev. Lett. **84**, 1800 (2000).
[11] J. P. Hill, B. J. Sternlieb, D. Gibbs, C. Detlefs, A. I. Goldman, C. Stassis, P. C. Canfield, and B. K. Cho, Phys. Rev. B **53**, 3487 (1996).
[12] C. D. Dewhurst, R. A. Doyle, E. Zeldov, and D. McK. Paul, Phys. Rev. Lett. **82**, 827 (1999).
[13] A. Dertinger, A. Kreyssig, C. Ritter, M. Loewenhaupt, and H. F. Braun, Physica B **284&288**, 485 (2000).
[14] L. P. Le, R. H. Heffner, J. D. Thompson, D. E. MacLaughlin, G.

J. Nieuwenhuys, A. Amato, R. Feyerherm, F. N. Gygax, A. Schenck, P. C. Canfield, and B. K. Cho, Phys. Rev. B **53**, 510 (1996).
[15] L. J. Chang, C. V. Tomy, D. McK. Paul, and C. Ritter, Phys. Rev. B **54**, 9031 (1996).
[16] B. Sternlieb, C. Stassis, A. I. Goldman, P. C. Canfield, and S. Shapiro, J. Appl. Phys. **81**, 4937 (1997).
[17] J. W. Lynn, S. Skanthakumar, Q. Huang, S. K. Sinha, Z. Hossain, L. C. Gupta, R. Nagarajan, and C. Godart, Phys. Rev. B **55**, 6584 (1997).
[18] K. Norgaard, M. R. Eskildsen, N. H. Andersen, J. Jensen, P. Hedegard, S. N. Klausen, and P. C. Canfield, Phys. Rev. Lett. **84**, 4982 (2000).
[19] S. K. Sinha, J. W. Lynn, T. E. Grigereit, Z. Hossain, L. C. Gupta, R. Nagarajan, and C. Godart, Phys. Rev. B **51**, 681 (1995).
[20] J. Zarestky, C. Stassis, A. I. Goldman, P. C. Canfield, P. Dervenagas, B. K. Cho, and D. C. Johnston, Phys. Rev. B **51**, 678 (1995).
[21] S. M. Choi, J. W. Lynn, D. Lopez, P. L. Gammel, P. C. Canfield, and S. L. Bud'ko, Phys. Rev. Lett. **87**, 107001 (2001).
[22] C. Detlefs, A. H. M. Z. Islam, T. Gu, A. I. Goldman, C. Stassis, P. C. Canfield, J. P. Hill, and T. Vogt, Phys. Rev. B **56**, 7843 (1997).
[23] J. Y. Rhee, X. Wang, and B. N. Harmon, Phys. Rev. B **51**, 15 585 (1995).
[24] R. Szymczak, H. Szymczak, L. Gladczuk, and M. Baran, J. Magn. Magn. Mater. **157&158**, 706 (1996).
[25] H. Kawano-Furukawa, H. Takeya, and K. Kadowaki, J. Magn. Magn. Mater. **226&230**, 278 (2001).
[26] H. Kawano-Furukawa, H. Takeshita, M. Ochiai, T. Nagata, H. Yoshizawa, N. Furukawa, H. Takeya, and K. Kadowaki, Phys. Rev. B **65**, 180508 (2002).
[27] P. L. Gammel, B. Barber, D. Lopez, A. P. Ramirez, D. J. Bishop, S. L. Bud'ko, and P. C. Canfield, Phys. Rev. Lett. **84**, 2497 (2000).
[28] H. Schmidt and H. F. Braun, Phys. Rev. B **55**, 8497 (1997).
[29] J. W. Lynn, Q. Huang, A. Santoro, R. J. Cava, J. J. Krajewski, and W. F. Peck, Phys. Rev. B **53**, 802 (1996).
[30] Q. Huang, J. W. Lynn, A. Santoro, B. C. Chakoumakos, R. J. Cava, J. J. Krajewski, and W. F. Peck, Physica C **271**, 311 (1996).
[31] S. L. Bud'ko, M. El Massalami, M. B. Fontes, J. Mondragon, W. Vanoni, B. Giordanengo, and E. M. Baggio-Saitovitch, Physica C **243**, 183 (1995).
[32] P. Bonville, J. A. Hodges, C. Vaast, E. Alleno, C. Godart, L. C. Gupta, Z. Hossain, and R. Nagarajan, Physica B **223&224**, 72 (1996).
[33] E. Alleno, P. Berger, E. Leroy, and C. Godart, in *Rare Earth Transition Metal Borocarbides (nitrides): Superconducting, Magnetic and Normal State Properties*, Vol. 14 of *NATO Science Series*, edited by K. H. Müller and V. N. Narozhnyi (Kluwer, Dordrecht, 2001), p. 265.
[34] J. Rodriguez-Carvajal, Physica B **192**, 55 (1993).
[35] V. F. Sears, Neutron News **3**, 26 (1992).
[36] P. Thompson, D. E. Cox, and J. B. Hastings, J. Appl. Crystallogr. **20**, 79 (1987).
[37] E. Alleno, S. Vivet, C. Godart, and E. Leroy (unpublished).
[38] W. E. Pickett and D. J. Singh, Phys. Rev. Lett. **72**, 3702 (1994).
[39] L. F. Mattheiss, Phys. Rev. B **49**, 13 279 (1994).
[40] R. Coehoorn, Physica C **228**, 331 (1994).
[41] J. van Duijn, J. P. Attfield, and K. Suzuki, Phys. Rev. B **62**, 6410 (2000).
[42] P. Bonville, J. A. Hodges, C. Vaast, E. Alleno, C. Godart, L. C. Gupta, Z. Hossain, R. Nagarajan, G. Hilscher, and H. Michor, Z. Phys. B: Condens. Matter **101**, 511 (1996).
[43] A. M. Mulders, P. C. M. Gubbens, U. Gasser, C. Baines, and K. H. J. Buschow, Phys. Rev. B **57**, 10 320 (1998).
[44] J. Jensen, Phys. Rev. B **65**, 140514 (2002).
[45] D. R. Sanchez, H. Micklitz, M. B. Fontes, S. L. Bud'ko, and E. Baggio-Saitovitch, Phys. Rev. Lett. **76**, 507 (1996).
[46] E. Tominez, E. Alleno, C. Godart, P. Bonville, and J. A. Hodges, J. Alloys Compd. **262&263**, 462 (1997).
[47] K. Machida, K. Nokura, and T. Matsubara, Phys. Rev. B **22**, 2307 (1980).
[48] S. V. Shulga, S. L. Drechsler, G. Fuchs, K. H. Möller, K. Winzer, M. Heinecke, and K. Krug, Phys. Rev. Lett. **80**, 1730 (1998).